JOC Article
pubs.acs.org/joc

Theoretical Investigations of the Photochemical Isomerizations of Indoxazene and Isoxazole

Ming-Der Su*

Department of Applied Chemistry, National Chiayi University, Chiayi 60004, Taiwan

midesu@mail.ncyu.edu.tw

Received May 19, 2009

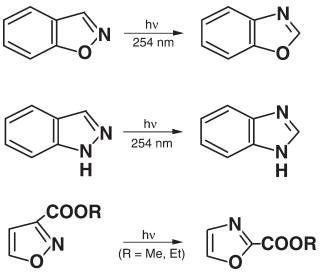

The mechanisms of the photochemical isomerization reactions were investigated using two model systems of indoxazene (**1**) and isoazole-3-carboxylate (**5**) with the CASSCF and MP2-CAS methods using the 6-311G(d,p) basis set. The active space of the former consists of 14 electrons in 11 orbitals, while that of the latter consists of 10 electrons in seven orbitals. Two reaction pathways were examined in the present work. They are referred to as the internal cyclization−isomerization path (paths I and III) and the direct path (paths II and IV). Our model investigations suggest that the preferred reaction route for these species is as follows: reactant → Franck−Condon region → conical intersection → photoproduct. In particular, the direct (conical intersection) mechanism found in this work gives a better explanation than the previous proposed mechanism and also supports the available experimental observations. Additionally, a simple p−π orbital topology model is proposed that can be used as a diagnostic tool to predict the location of the conical intersections as well as the geometries of the phototransposition products of various heterocycles.

I. Introduction

Studies of the photochemical isomerizations of five- and six-membered heterocyclic ring compounds have received considerable attention in recent years.[1] The majority of reactions studied are those involving an interchange of two adjacent ring atoms.[2] Many experiments and theoretical investigations have been carried out in order to derive the mechanisms involved.[1,2] Nevertheless, due to the great diversity of photoreactions, theoretical investigations of such reactions have been carried out less often than experimental studies, and calculations to date have mainly been performed for small molecules.

Ferris and Antonucci performed an extensive study of photoisomerization reactions in ortho-substituted benzene and related hetercycles.[3] They reported that irradiation of indoxazene (**1**) at 254 nm can produce benzoxazole (**2**) as a result of the interchange of adjacent ring atoms.[4] See Scheme 1a. However, no intermediate could be detected in this conversion. The solvent dependence of the reaction suggests that **2** is formed from an initial π,π^* excitation. Moreover, quenching and sensitization studies indicate that the formation of **2** proceeds from the singlet state. Similarly, it was observed that irradiation of indazole (**3**) in the liquid phase yields benzimidazole (**4**).[4] See Scheme 1b. Besides these, Good and Jones were the first to show that isoazole-3-carboxylate (**5**) and its analogue rearrange photochemically to

(1) For reviews, see: (a) Horspool, W. In *Organic Photochemistry: A Comprehensive Treatment*; Simon & Schuster: London, 1992. (b) Kopecky, J. In *Organic Photochemistry: A Visual Approach*; VCH Publishers: New York, 1992.

(2) For instance, see: (a) De Mayo, P. In *Rearrangements in Ground and Excited States*; Academic Press: New York, 1980; Vol. 3. (b) Buchardt, O. In *Photochemistry of Heterocyclic Compounds*; Wiley: New York, 1976.

(3) (a) Ferris, J. P.; Antonucci, F. R.; Trimmer, R. W. *J. Am. Chem. Soc.* **1973**, *95*, 919. (b) Ferris, J. P.; Antonucci, F. R. *J. Am. Chem. Soc.* **1974**, *96*, 2010.

(4) Ferris, J. P.; Antonucci, F. R. *J. Am. Chem. Soc.* **1974**, *96*, 2014.

DOI: 10.1021/jo901010q Published on Web 07/20/2009

the corresponding oxazole-2-carboxylate (**6**) isomers.[5] See Scheme 1c.

As can be seen from Scheme 1, these experimental studies show a similar photochemical pattern. That is, the photochemical rearrangements of **1**, **3**, and **5** take place with major reorganization of the five-membered ring. The results of these experiments allow the postulation of mechanisms which can rationalize the experimental findings. In fact, an understanding of the detailed mechanism of such transformations is essential to the rationalization of the mechanisms of intramolecular photochemical valence isomerizations, which are useful in synthetic chemistry. Knowledge of the positions of the heteroatoms in the five-membered ring after rearrangement would greatly aid the mechanistic interpretation. However, to the best of our knowledge, no theoretical study has been reported for such photochemical reactions. A theoretical study of the photoisomerization of both indoxazene (**1**) and isoazole-3-carboxylate (**5**) was thus undertaken.

As far as we are aware, one mechanism has been proposed to rationalize the rearrangement patterns of indoxazene (**1**), indazole (**3**), and isoazole-3-carboxylate (**5**). This mechanism is the so-called internal cyclization−isomerization mechanism.[2a] It involves the initial formation of a bicyclic isomer followed by a [1,3] migration of the nitrogen atom to a second bicyclic isomer, which then undergoes a ring-opening to the rearranged product. However, as mentioned previously, no intermediate has been detected during such photoisomerization reactions,[4] and as a result, this mechanism cannot account for all of the experimental observations found in the **1**, **3**, and **5** systems. Thus, a second mechanism was considered: the direct (conical intersection) mechanism to rationalize the experimental results.

The object of the present work is an understanding of the photochemical mechanism of the transformation of indoxazene (**1**) to benzoxazole (**2**), indazole (**3**) to benzimidazole (**4**), as well as isoazole-3-carboxylate (**5**) to oxazole-2-carboxylate (**6**). As illustrated in Scheme 1, the reaction mechanisms of these photochemical reactions were investigated by CASSCF (complete-active-space SCF) and MP2-CAS calculations. Due to the similarity between species **1** and **3**, only **1** and **5** were used as model systems in the present study. In the following sections, the method is described and the results are presented for these phototransposition reactions in detail. Conical intersection regions[6] on the potential surface, where decay to the ground-state surface can occur, have been located, and ground-state reaction paths leading from these conical intersections to a variety of products have been identified. On the basis of this information, the reaction process is explained. It will be shown below that conical intersections[6] play a crucial role in the photoisomerization reactions of these aromatic systems.

II. Methodology

All geometries were fully optimized without imposing any symmetry constraints, although in some instances the resulting structures showed various elements of symmetry. The CASSCF calculations were performed using the MCSCF program released in GAUSSIAN 03.[7]

SCHEME 1

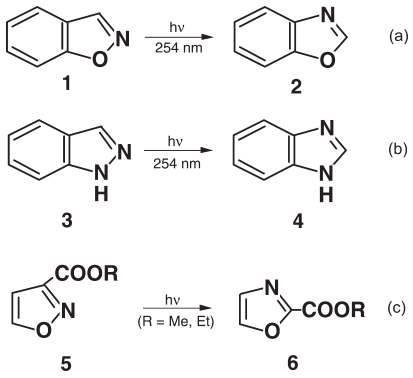

In the investigation of the photochemical reaction pathways, the stationary point structures on the S_0 and S_1 surfaces were optimized at the CASSCF level of calculation using the standard 6-311G(d) basis set.[8] The active space for describing the photoisomerizations of **1** comprises 14 electrons in 11 orbitals, i.e., nine p−π orbitals plus two nonbonding orbitals, which is referred to as CASSCF(14,11). The active space for describing the photoisomerizations of **5** comprises 10 electrons in seven orbitals, i.e., five p−π orbitals plus two nonbonding orbitals, which is referred to as CASSCF(10,7). The state-averaged CASSCF(14,11) and CASSCF(10,7) methods were used to determine the geometry on the intersection space. The optimization of the conical intersections was achieved in the (*f*-2)-dimensional intersection space using the method of Bearpark et al.[9] implemented in the Gaussian 03 program.[7]

Every stationary point was characterized by its harmonic frequencies computed analytically at the CASSCF level. The harmonic vibrational frequencies of all stationary points were computed analytically to characterize them as either minima (all frequencies are real) or transition states (only one imaginary frequency). The optimization was determined when the maximum force and its root-mean-square (rms) were less than 0.00045 and 0.00005 hartree/bohr, respectively. Localization of the minima, transition states, and conical intersection minima was performed in Cartesian coordinates; therefore, the results are independent of any specific choice of internal variables.

To correct the energetics for dynamic electron correlation, the multireference Møller−Plesset algorithm[10] as implemented in

(5) Good, R. H.; Jones, G. *J. Chem. Soc. C* **1971**, 1196.

(6) For recently excellent reviews, see: (a) Bernardi, F.; Olivucci, M.; Robb, M. A. *Isr. J. Chem.* **1993**, 265. (b) Klessinger, M. *Angew. Chem., Int. Ed. Engl.* **1995**, *34*, 549. (c) Bernardi, F.; Olivucci, M.; Robb, M. A. *Chem. Soc. Rev.* **1996**, 321. (d) Bernardi, F.; Olivucci, M.; Robb, M. A. *J. Photochem. Photobiol. A: Chem.* **1997**, *105*, 365. (e) Klessinger, M. *Pure Appl. Chem.* **1997**, *69*, 773. (f) Klessinger, M.; Michl J. *Excited States and Photochemistry of Organic Molecules*; VCH Publishers: New York, 1995.

(7) Frisch, M. J.; Trucks, G. W.; Schlegel, H. B.; Scuseria, G. E.; Robb, M. A.; Cheeseman, J. R.; Zakrzewski, V. G.; Montgomery, J. A., Jr.; Vreven, T.; Kudin, K. N.; Burant, J. C.; Millam, J. M.; Iyengar, S. S.; Tomasi, J.; Barone, V.; Mennucci, B.; Cossi, M.; Scalmani, G.; Rega, N.; Petersson, G. A.; Nakatsuji, H.; Hada, M.; Ehara, M.; Toyota, K.; Fukuda, R.; Hasegawa, J.; Ishida, M.; Nakajima, T.; Honda, Y.; Kitao, O.; Nakai, H.; Klene, M.; Li, X.; Knox, J. E.; Hratchian, H. P.; Cross, J. B.; Adamo, C.; Jaramillo, J.; Gomperts, R.; Stratmann, R. E.; Yazyev, O.; Austin, A. J.; Cammi, R.; Pomelli, C.; Ochterski, J. W.; Ayala, P. Y.; Morokuma, K.; Voth, G. A.; Salvador, P.; Dannenberg, J. J.; Zakrzewski, V. G.; Dapprich, S.; Daniels, A. D.; Strain, M. C.; Farkas, O.; Malick, D. K.; Rabuck, A. D.; Raghavachari, K.; Foresman, J. B.; Ortiz, J. V.; Cui, Q.; Baboul, A. G.; Clifford, S.; Cioslowski, J.; Stefanov, B. B.; Liu, G.; Liashenko, A.; Piskorz, P.; Komaromi, I.; Martin, R. L.; Fox, D. J.; Keith, T.; Al-Laham, M. A.; Peng, C. Y.; Nanayakkara, A.; Challacombe, M.; Gill, P. M. W.; Johnson, B.; Chen, W.; Wong, M. W.; Gonzalez, C.; Pople, J. A. Gaussian, Inc., Wallingford CT, 2003.

(8) Hehre, W. J.; Radom, L.; Schleyer, P. v. R.; Pople, J. A. *Ab Initio Molecular Orbital Theory*; Wiley: New York, 1986.

(9) Bearpark, M. J.; Robb, M. A.; Schlegel, H. B. *Chem. Phys. Lett.* **1994**, *223*, 269.

(10) McDouall, J. J. W.; Peasley, K.; Robb, M. A. *Chem. Phys. Lett.* **1988**, *148*, 183.

SCHEME 2

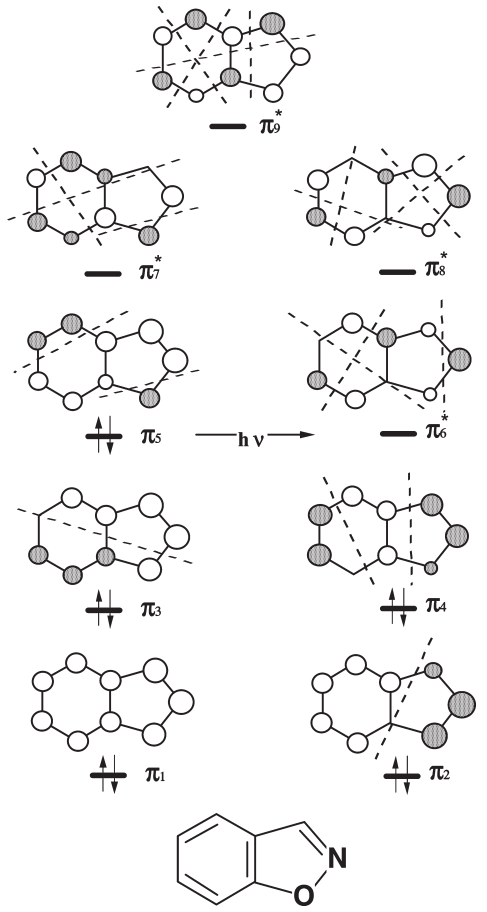

SCHEME 3

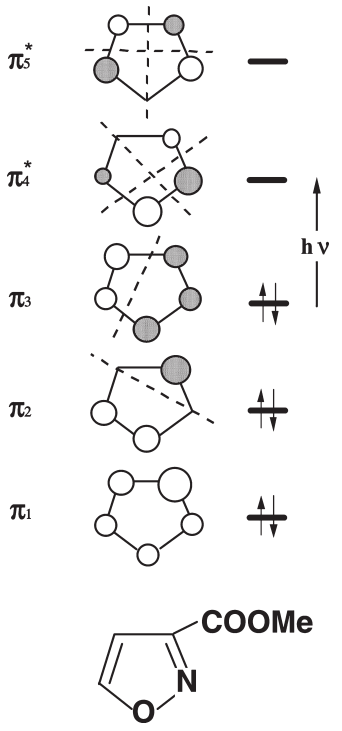

the program package GAUSSIAN 03 has been used. Unless otherwise noted, the relative energies given in the text are those determined at the MP2-CAS-(10,7)/6-311G(d,p) and MP2-CAS-(14,11)/6-311G(d,p) levels using the CAS(10,7)/6-311G(d) and CAS(14,11)/6-311G(d) (hereafter designed MP2-CAS and CASSCF, respectively) geometries, respectively.

III. General Considerations

As mentioned in the Introduction, it was reported that for **1** experimentalists have found no indication for the participation of a triplet state.[4] Triplet states therefore play no role in the reactions studied in the present work. Also, in one experimental study performed by Ferris and Antonucci,[4] it was found that **2** is formed from the $\pi \rightarrow \pi^*$ excitation. For these reasons, the photochemical transposition reactions of indoxazene (**1**) should proceed on singlet surfaces and also should only involve the $\pi \rightarrow \pi^*$ transition.[12] Thus, the focus shall be on $^1(\pi, \pi^*)$ surfaces from now on.

Furthermore, the electronic structures of indoxazene (**1**) and isoazole-3-carboxylate (**5**) are now analyzed, which form the basis for this study. General outlines of the nine p−π orbitals in **1** and five p−π orbitals in **5** are shown explicitly in Schemes 2 and 3, respectively. As can be seen, the lowest singlet $\pi \rightarrow \pi^*$ excitations for **1** and **5** are the singlet π_5 (HOMO) → π_6^* (LUMO) and singlet π_3 (HOMO) → π_4^* (LUMO) transitions, respectively. It is worth noting that the mixing of π and π^* levels redistributes the electron density. As a consequence, in the perturbed HOMO level, the electron density (from the atomic orbital coefficients) is increased on the two *o*-nitrogen and carbon atoms. On the other hand, the coefficients at the two ortho positions increased in the perturbed LUMO level.

The central novel feature of the photochemical mechanisms of **1** and **5** is the location of conical intersections in the excited- and ground-electronic states. In the present work, the p−π orbital model as outlined in Schemes 2 and 3 is used to search for the conical intersections (the direct mechanism) of the photoisomerizations of the **1** and **5** molecules. Figure 1 shows the qualitative potential energy surfaces for the S_0 and S_1 states of **1** and **5** as a function of rotation about the N=C double bond (i.e., the rotation angle θ).[11] By twisting the N=C π bond in **1** or **5**, both π_5, π_6^* and π_3, π_4^* are raised in energy due to increased antibonding interactions. Consequently, these π orbitals become degenerate at a geometry around 65° for both **1** (path II; vide infra) and **5** (path IV; vide infra), as shown in Figure 1. In other words, this excitation removes the barrier to rotation about the former N=C axis. Besides, rotation toward an out-of-plane orientation of the p−π orbitals lowers the energy of the excited state. Although these out-of-plane angles were obtained without full optimization of the reactant, they at least give us a hint that a degeneracy between HOMO and LUMO can exist as a result of the rotation of a single N=C bond. Moreover, the formation of such a degenerate point provides further

(11) The C−C, C−N, C−H, C−O, and N−O bonds in **1** and **5** are fixed to be 1.35, 1.30, 1.09, 1.30, and 1.30 Å, respectively. Also, the ∠CCC (for six-membered ring), ∠CCC, ∠CNC, ∠HCC, ∠HNC, ∠CON, and ∠CCN bond angles are fixed to be 120°, 108°, 108°, 126°, 126°, 108°, and 180°, respectively.

(12) For the assignment of calculated excitations to the band of the UV spectrum, the calculated oscillator strengths were also used. It shows that the crucial excitation for the two photochemical reactions can only go to the one close-lying state of $\pi-\pi^*$ type with appreciable oscillator strengths of magnitude 10^{-2}. However, experimental data are not available for them.

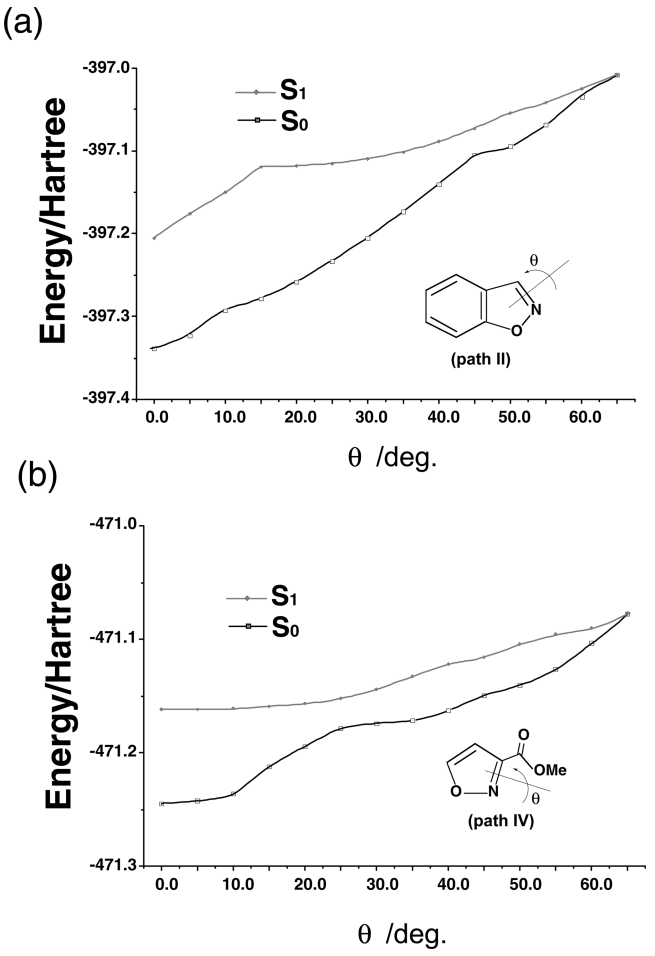

FIGURE 1. Minimum-energy pathways of indoxazene (**1**; above) and isoazole-3-carboxylate (**5**; below) along the torsion angle coordinate optimized for the S_1 state at the (a) CAS(14,11)/6-311G(d) and (b) CAS(10,7)/6-311G(d) levels of theory.

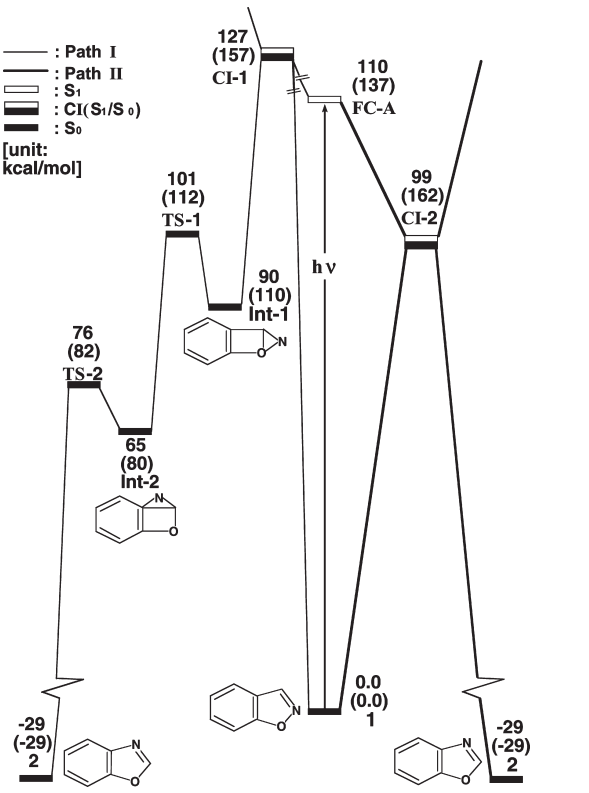

FIGURE 2. Energy profiles for the photoisomerization modes of indoxazene (**1**). The abbreviations FC and CI stand for Franck−Condon and conical intersection, respectively. The relative energies were obtained at the MP2-CAS-(14,11)-6-311G(d,p)//CAS(14,11)/6-311G(d) and CAS(14,11)/6-311G(d) (in parentheses) levels of theory. All energies (in kcal/mol) are given with respect to the reactant (**1**). For the CASSCF-optimized structures of the crucial points, see Figure 3. For more information, see the text.

evidence for an enhanced intramolecular rotation in the five-membered ring geometry, and possibly the existence of a conical intersection, where decay to the ground state can be fully efficient. Accordingly, the above results are used to interpret the mechanisms for the photochemical isomerization reactions of **1** and **5** in the following section.

IV. Results and Discussion

(**1**)**. Indoxazene.** First, the photoisomerization of indoxazene (**1**) as indicated in Scheme 1a is considered. According to the discussion above, there could be two kinds of reaction pathways for photorearrangement on the singlet excited potential energy surface of **1**. That is, an internal cyclization−isomerization pathway (path I) and a direct pathway (path II), which both lead to the same photoproduct, benzoxazole (**2**). Figure 2 contains all the relative energies of the various points with respect to the energy of the reactant **1**. In addition, these relative energies obtained using both CASSCF and MP2-CAS methods are collected in Table 1 (Supporting Information). The structures of the various critical points on the possible mechanistic pathways of Figure 2 are demonstrated in Figure 3. Cartesian coordinates and energetics calculated for the various points using both methods are available as Supporting Information.

In the first step, the reactant (indoxazene, **1**) is promoted to its excited singlet state by a vertical excitation as shown in the middle of Figure 2. Our CASSCF and MP2-CAS vertical excitation energies to the lowest excited π^* state of **1** were calculated to be 137 and 110 kcal/mol, respectively. After the vertical excitation process, the molecule is situated on the excited singlet surface but still possesses the S_0 (ground-state) geometry (**FC-A**). As discussed in the previous section, the calculated 110 kcal/mol band for **1** is best described as the $\pi_5 \rightarrow \pi_6^*$ transition. Accordingly, our computational results confirm that the only excited state involved in the photorearrangement of indoxazene (**1**) is the singlet (π, π^*).[12]

From the point reached by the vertical excitation, the molecule relaxes to reach an S_1/S_0 CI where the photoexcited system decays nonradiatively to S_0. Specifically, the photochemically active relaxation path, starting from the S_1 $^1(\pi_5 \rightarrow \pi_6^*)$ excited state of **1**, leads to S_1/S_0 **CI-1** (path I) or **CI-2** (path II). These paths are shown in the left- and right-hand side of Figure 2, respectively. Both these conical intersection structures optimized at the CASSCF/6-311G(d) level are collected in Figure 3. The derivative coupling and gradient

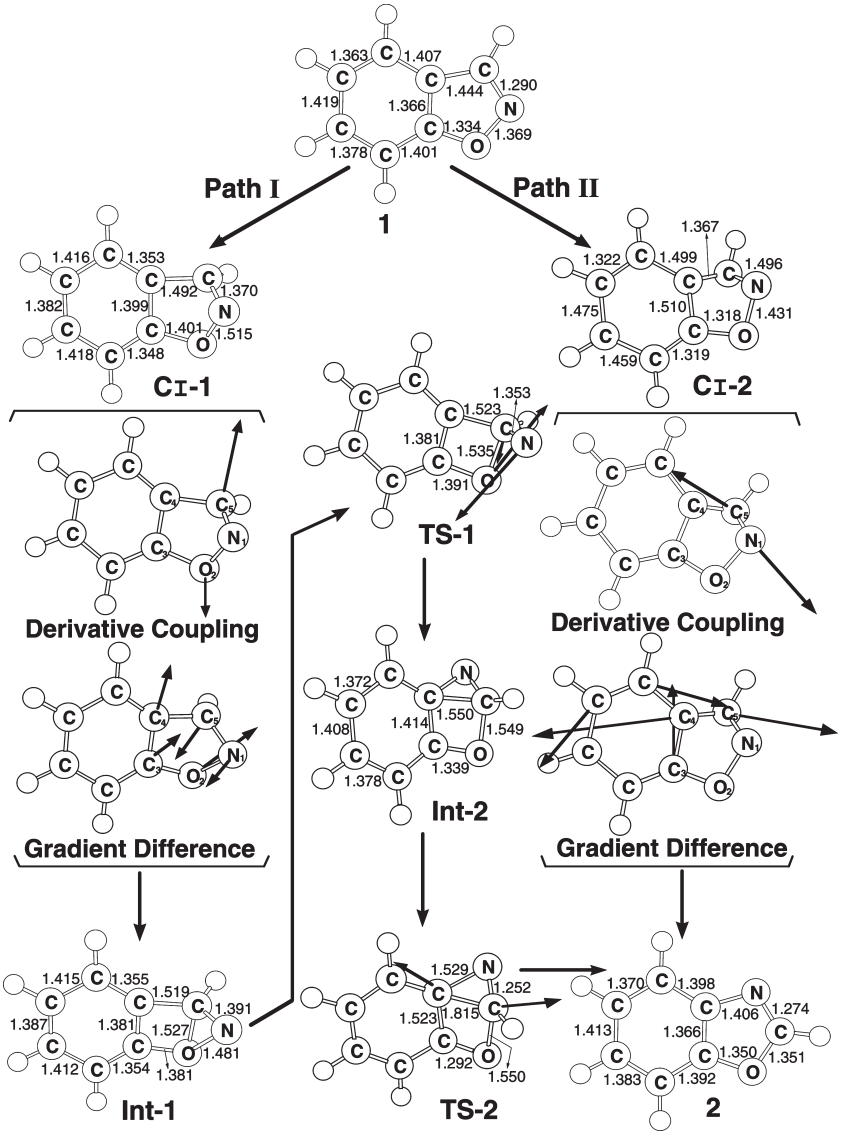

FIGURE 3. CAS(14,11)/6-311G(d) geometries (in Å and deg) for paths I and II of indoxazene (**1**),conical intersection (CI), intermediate (Int), transition state (TS), and isomer products. The derivative coupling and gradient difference vectors—those which lift the degeneracy—computed with CASSCF at the conical intersections **CI-1** and **CI-2**. The corresponding CASSCF vectors are shown in the inset. For more information, see the Supporting Information.

difference vectors obtained at these conical intersections are also represented in Figure 3.[13]

The S_1/S_0 conical intersection **CI-1** will be discussed first. From the structure of **CI-1**, the nature of the relaxation path on the S_1 potential surface is regarded as the $O-C_1$ bond formation. As can be seen in Figure 2, our theoretical findings suggest that the energy of **CI-1** lies 127 kcal/mol above **1** and 17 kcal/mol higher in energy than **FC-A**. Funneling through the conical intersection, different reaction pathways on the ground-state surface may be predicted by following the derivative coupling vector or the gradient difference vector direction.[6] As demonstrated in Figure 3, the major contribution of the derivative coupling vector involves the O_2-C_5 bond formation motion, while the gradient difference vector corresponds to the C_4-C_5 and C_3-O_2 bonds bending motion that leads to a vibrationally hot $1-S_0$ species.

As a consequence, following the derivative coupling vector from S_1/S_0 **CI-1** (Figure 2) leads to the formation of bicyclic intermediate **Int-1**. This intermediate is nonplanar, the nitrogen atom being bent out of the ring plane by an angle of about 54°. The local minimum **Int-1** is calculated to be

(13) One reviewer pointed out that, in the CAS energies, both CI-1 and CI-2 are higher than FC-A, while in the MP2 energies CI-2 is much lower than FC-A. The reason for such a difference could be because this MP2 geometry is very different from its CASSCF geometry. On the other hand, if the bigger active space and the bigger basis sets are chosen, better computational results may be obtained. However, as far as we know, no computational software is available for fully optimizing the MP2 geometry. Thusthe better conical intersection structures based on the MP2(CAS) method cannot be obtained. Moreover, it is pointed out in Figure 2 that a much higher excitation energy of about 127 kcal/mol for reactant **1**, which lies outside the range of the singlet vertical energy (110 kcal/mol), is calculated. Even if the error bar for the computed excitation energies that may lower the position of the singlet state is taken into account, it can be expected that the singlet vertical energy would not be sufficient to induce $S_0 \rightarrow S_1$ excitation for such compounds. In brief, the present computations can at least give the qualitative results and explanations for understanding their photochemical mechanisms.

37 kcal/mol lower than that of **CI-1** but is 90 kcal/mol higher than that of the reactant **1**. The next reaction step is a [1,3] sigmatropic shift of the nitrogen atom from O_2 to C_4, which takes place through transition state **TS-1** in Figure 2. Normal-mode analysis confirms that this structure has one imaginary frequency, $408i$ cm^{-1}, and IRC calculations indicate that **TS-1** connects **Int-1** with **Int-2**. The barrier height at **TS-1** measured from **Int-1** is 11 kcal/mol. Once **Int-2** is formed, a four-membered ring-opening by C−C bond activation can take place via the transition state **TS-2**, which is located 11 kcal/mol above **Int-2** and leads to the final photoproduct **2**. It should be pointed out that the energy required to overcome the barrier at **TS-2** is small, 11 kcal/mol, and it is much less than the energy difference of 37 kcal/mol between **Int-1** and **CI-1**. That is to say, the **1** molecule possesses an excess energy of around 35 kcal/mol arising from the relaxation to the local minimum **Int-1**, which is greater than the energy difference between **Int-1** and **TS-1** (11 kcal/mol) and **Int-2** and **TS-2** (11 kcal/mol). As a consequence, the reactant molecule can easily cross over the TS-1 and **TS-2** barriers to form the final product, **2**. Our computational results thus suggest that the mechanism for path I should proceed as follows:

$$\text{path I}: \mathbf{1} \rightarrow \mathbf{FC\text{-}A} \rightarrow \mathbf{S_1/S_0CI\text{-}1} \rightarrow \mathbf{Int\text{-}1} \rightarrow \mathbf{TS\text{-}1} \rightarrow \mathbf{Int\text{-}2} \rightarrow \mathbf{TS\text{-}2} \rightarrow \mathbf{2}$$

On the other hand, the mechanism of path II, which contains only a single conical intersection point (S_1/S_0 **CI-2**), can now be explored. The derivative coupling and gradient difference vectors obtained at the conical intersection are given in Figure 3. As one can see, the MP2-CAS results suggest that S_1/S_0 **CI-2** is lower in energy than **FC-A** by 11 kcal/mol, while the competing S_1/S_0 **CI-1** is higher in energy than S_1/S_0 **CI-2** by 28 kcal/mol. The existence of a low-lying conical intersection provides a highly effective radiationless decay channel.[6] Additionally, our present computational results demonstrate that the path II channel is a one-step process, which only involves the S_1/S_0 **CI-2** point. Consequently, our model calculations indicate that path II is more favorable than path I from both energetic and practical viewpoints. Also, the computations predict that the photochemical rearrangement reaction of path II should be a barrierless process. That is, starting from the **FC-A** point, indoxazene (**1**) enters an extremely efficient decay channel, S_1/S_0 **CI-2**. After decay at this conical intersection point, the photoisomer **2** as well as the initial reactant **1** can be reached via a barrierless ground-state relaxation pathway. Accordingly, the process of path II can be represented as follows:

$$\text{path II}: \mathbf{1} \rightarrow \mathbf{FC\text{-}1} \rightarrow \mathbf{S_1/S_0CI\text{-}2} \rightarrow \mathbf{2}$$

In brief, our model investigations demonstrate that upon absorption of a photon of light, indoxazene (**1**) is excited vertically to S_1 (**FC-A**). From this point, the system can return to the ground state via two radiationless decay routes (paths I and II). The present calculations indicate that path I is quite inefficient because it involves multiple steps to obtain the final photoproduct, compared with a single step for path II. Moreover, path I involves two intermediates, which were not found in the available experimental observations.[4] In fact, the presence of excited state intermediates along the path allows for redistribution of the photon energy. Besides this, the energetic requirement of the multiple steps of path I is greater than that of the single step of path II. Indeed, for path II, **1** in the S_1 state proceeds to rotate one N−C bond via a conical intersection and, subsequently, returns to the ground state nonradiatively to give benzoxazole (**2**) without any intermediates. This results in **2** as the only major product. In consequence, all of these results strongly suggest that path II should be much more favorable than path I. All these theoretical findings are in accordance with the experimental findings.[4]

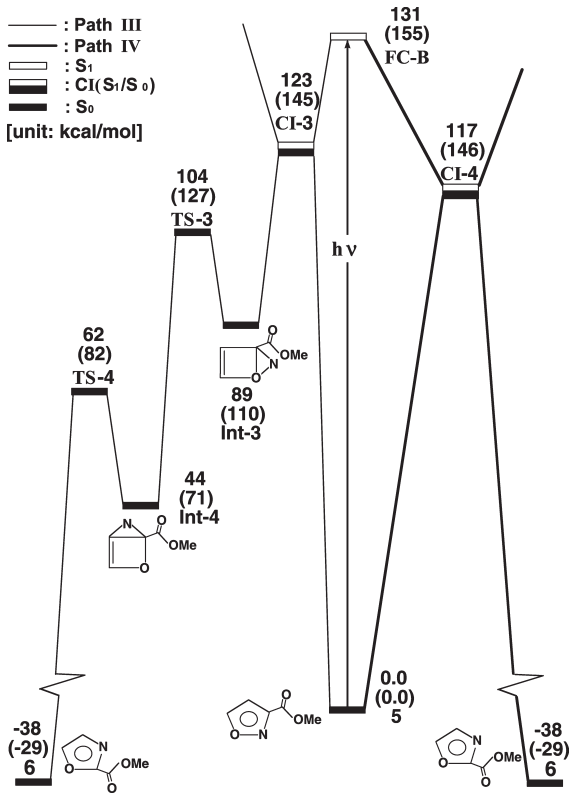

FIGURE 4. Energy profiles for the photoisomerization modes of isoazole-3-carboxylate (**5**). The abbreviations FC and CI stand for Franck−Condon and conical intersection, respectively. The relative energies were obtained at the MP2-CAS-(10,7)/6-311G(d,p)//CAS(10,7)/6-311G(d) and CAS(14,11)/6-311G(d) (in parentheses) levels of theory. All energies (in kcal/mol) are given with respect to the reactant (**5**). For the CASSCF-optimized structures of the crucial points, see Figure 5. For more information, see the text.

(**2**)**. Isoazole-3-carboxylate.** Next, the photoisomerization of isoazole-3-carboxylate (**5**) as indicated in Scheme 1c is considered. As discussed previously, there are two reaction pathways as follows: an internal cyclization−isomerization pathway (path III) and a direct pathway (path IV). These pathways can both lead to the same photoproduct, oxazole-2-carboxylate (**6**). In this section, these two reaction routes for **5** are compared. The entire potential energy surface is summarized in Figure 4, and conclusions concerning the mechanisms studied in this work are made. The energetics of the intermediates, transition states, and conical intersections for these reactions are presented in Table 2 (Supporting Information). The structures of the various critical points on the mechanistic pathways of Figure 4 are collected in Figure 5. Cartesian coordinates and energetics calculated for

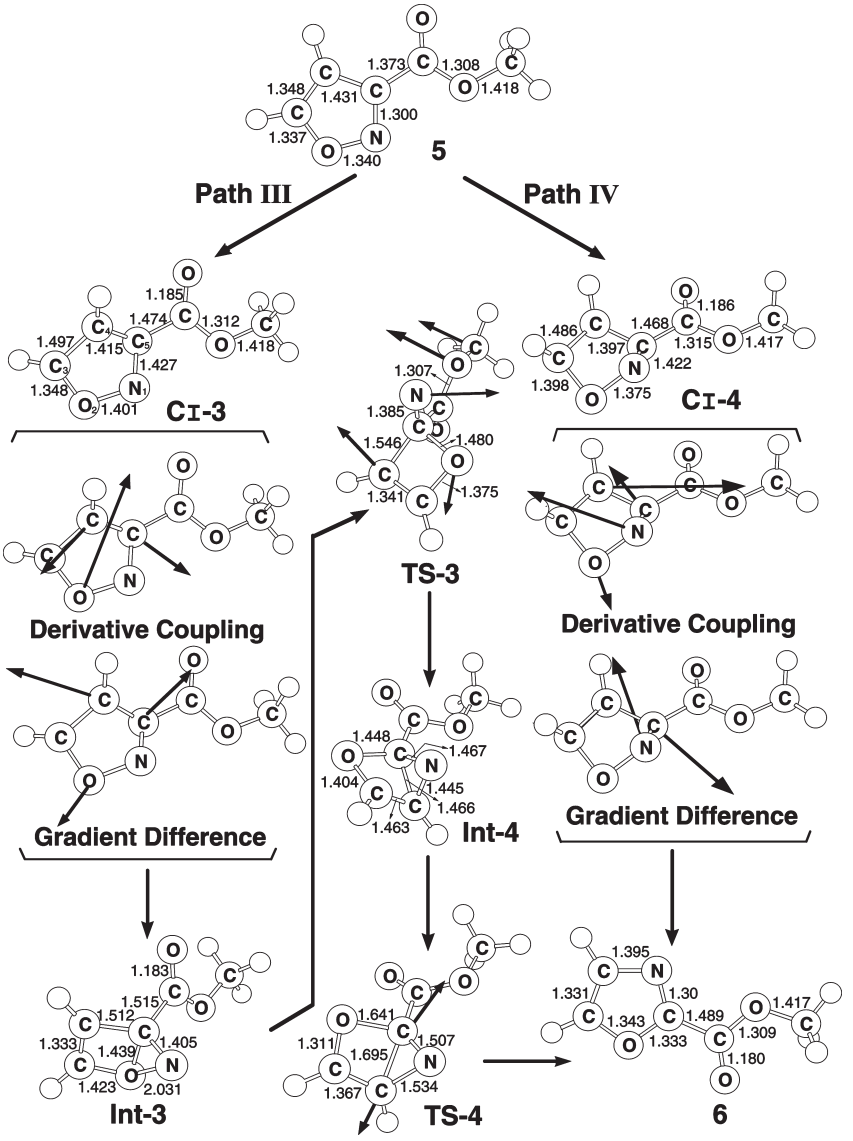

FIGURE 5. CAS(10,7)/6-311G(d) geometries (in Å and deg) for paths III and IV of isoazole-3-carboxylate (**5**), conical intersection (CI), intermediate (Int), transition state (TS), and isomer products. The derivative coupling and gradient difference vectors—those which lift the degeneracy—computed with CASSCF at the conical intersections **CI-3** and **CI-4**. The corresponding CASSCF vectors are shown in the inset. For more information, see the Supporting Information.

these points at both methods are available as Supporting Information.

Again, the reactant (isoazole-3-carboxylate, **5**) is initially promoted to its excited singlet state by a vertical excitation as shown in the middle of Figure 4. Our CASSCF and MP2-CAS vertical excitation energies to the lowest excited π^* state of **5** (**FC-B**) are calculated to be 155 and 131 kcal/mol, respectively.[12] As there are no relevant experimental and theoretical data for such a molecule,[5] the above result is a prediction.

As presented in Figure 4, in path III, geometry optimization on the S_1 ($\pi_3 \rightarrow \pi_4^*$) excited state was performed by bending the O_2---C_5 (1.780 Å) bond of **5**. The relaxation reaches S_1/S_0 **CI-3** where the photoexcited system decays nonradiatively to the ground-state (S_0). For comparison, the corresponding O_2---C_5 distance is 2.660 Å at the ground-state minimum **5**. As a result, the nature of the relaxation of **5** on the path III potential energy surface can be regarded as an O_2-C_5 bond closure. Moreover, according to the results outlined in Figure 4, funneling through S_1/S_0 **CI-3** leads to two different reaction paths on the ground-state surface, via either the derivative coupling vector or the gradient difference vector.[6] See Figure 5. The gradient difference vector for **CI-3** corresponds to an antisymmetric bending motion, which leads to a vibrationally hot species at the S_0 configuration. On the other hand, its derivative coupling vector corresponds to the intramolecular formation of a four-membered ring species. Indeed, following the derivative coupling vector from **CI-3** and decreasing the $N_1O_2C_5$ bond angle, the system arrives at a bicyclic local intermediate, **Int-3**. The optimized geometry of intermediate **Int-3**, shown in Figure 5, indicates that this structure has an N atom bending out of plane, while both O_2 and C_5 atoms connect to form the bicyclic ring. According to the MP2-CAS result, the energy of **Int-3** is 34 kcal/mol lower than that of the conical intersection **CI-3** but 89 kcal/mol higher than that of the reactant **5**.

The next reaction step of path III is the migration of the N atom leading to another bicyclic intermediate **Int-4** via **TS-3**. Our MP2-CAS calculations indicate that the bicyclic formation of **Int-4** from **Int-3** is exothermic by 45 kcal/mol and has an activation barrier of 15 kcal/mol. Once **Int-4** is formed, the C_4-C_5 bond activation can take place via transition state **TS-4**, which is 18 kcal/mol higher in energy than **Int-4**. That is, there is some interaction between C_4 and C_5 atoms, which is indicated by the C_4-C_5 distance of 1.695 Å. Normal-mode analysis shows a single imaginary frequency of $1052i$ cm^{-1}. The corresponding normal mode, shown in Figure 5, clearly demonstrates the five-membered ring character of the transition state. It is worth noting that the reactant molecule (**5**) possesses an excess energy of about 42 kcal/mol arising from the relaxation to the local intermediate **Int-3**, which is larger than the energy difference between **Int-4** and **TS-4** (18 kcal/mol). As a consequence, our model calculations demonstrate that, if the conical intersection **CI-3** is formed, the reactant molecule (**5**) could arrive at the final photoproduct, **6** without any difficulty. Accordingly, the present theoretical investigations suggest that path III for isoazole-3-carboxylate (**5**) can proceed as follows:

$$\text{path III}: \mathbf{5} \rightarrow \mathbf{FC\text{-}B} \rightarrow \mathbf{S_1/S_0CI\text{-}3} \rightarrow \mathbf{Int\text{-}3} \rightarrow \mathbf{TS\text{-}3} \rightarrow \mathbf{Int\text{-}4} \rightarrow \mathbf{TS\text{-}4} \rightarrow \mathbf{6}$$

The mechanism of path IV, which involves a single conical intersection point (S_1/S_0 **CI-4**). is considered next. That is to say, the path IV channel is a one−step process which only contains the S_1/S_0 **CI-4** point. Both derivative coupling and gradient difference vectors obtained at this conical intersection are depicted in Figure 5. Our MP2-CAS results estimate that S_1/S_0 **CI-4** is lower in energy than **FC-B** by 14 kcal/mol, while the competing S_1/S_0 **CI-3** is higher in energy than S_1/S_0 **CI-4** by 6.1 kcal/mol. Accordingly, our theoretical results demonstrate that the phototransposition reaction of path IV should be a nonradiative process. Similarly, after decay at this conical intersection point, the photoproduct **6** as well as the initial reactant **5** can be reached via a barrierless ground-state relaxation pathway. In consequence, the process of path IV can be given as follows:

$$\text{path IV}: \mathbf{5} \rightarrow \mathbf{FC\text{-}B} \rightarrow \mathbf{S_1/S_0CI\text{-}4} \rightarrow \mathbf{6}$$

In short, two mechanisms, paths III and IV, have been used to explore the photochemical transposition reactions of oxazole-2-carboxylate (**6**). It is found that the direct route (path IV) is the most favorable reaction pathway at both levels of calculations. The reason for this is simply because path IV is a one-step, low energy process, while the other mechanism (path III) is a multistep process with high activation barriers. It is also demonstrated that a back-reaction from product (**6**) to reactant (**5**) can be found in such photoisomerizations.[14]

(14) One reviewer of this paper mentioned the substituent effect of electron-withdrawing 3-carboxylate on the photochemistry. We agree that the influence of substituents may alter the position of the singlet state as well as the Franck−Condon region for such reactant species. This kind of investigation needs a great deal of both experimental and theoretical evidence as well as work. However, as one can see in the Introduction, to the best of our knowledge, no available experimental or theoretical observations about the related study have been reported. It is thus quite difficult for us to test such photochemical isomerization reactions theoretically, since there is no related experimental data available for comparison. Moreover, the theoretical investigations of the substituent effect on such compounds are beyond the scope of the present study. We have a continuing interest in such photochemical transposition reactions and will report computational studies of the substituent effect on such photoorganic systems in future publications.

V. Conclusion

The reaction mechanisms of the photoreactions of indoxazene (Scheme 1a) and isoazole-3-carboxylate (Scheme 1c), with respect to permutation of the ring atoms, have been studied. Taking all of the systems studied in this paper together, one can draw the following conclusions:

(1) If a heterocyclic molecule bearing electronegative atoms, such as the N and O atoms in this work, absorbs a photon to reach an excited singlet via a $^1(\pi \rightarrow \pi^*)$ transition, then this molecule will rotate a heterocyclic ring bond. This has the effect of decreasing the energy gap between the HOMO and the LUMO. As a result, this excited molecule can enter an extremely efficient channel, which takes the form of a conical intersection between the excited- and ground-state potential energy surfaces. After decay at the conical intersection point, the molecule continues its evolution on the ground-state potential surface to produce new chemical products.[6]

(2) Two important mechanisms, i.e., an internal cyclization−isomerization pathway (paths I and III) and a direct pathway (paths II and IV), have been considered to test the phototransposition reactions of indoxazene (**1**) and isoazole-3-carboxylate (**5**). It is found that the first mechanism consists of a sequence of small geometric rearrangements, which can either lead to the product or to a reformation of the reactant. Nevertheless, our theoretical findings strongly suggest that the direct pathway (paths II and IV) is always the most favorable reaction route. For the direct pathway, the reactants (i.e., **1** and **5**) in the S_1 state proceed to rotate one N=C bond via a conical intersection point and, subsequently, return to the ground state nonradiatively to give photoproducts (i.e., **2** and **6**, respectively) without producing any intermediates. That is, our theoretical results demonstrate that the direct pathway is more favorable from both energetic and kinetic viewpoints.

(3) The internal cyclization−isomerization mechanisms (paths I and III) involve several high energy transition structures, which make them unfeasible from a kinetic point of view. Also, this pathway is a multistep process which involves several intermediates. However, as stated in the introduction, no intermediates have been found in the available experimental observations.[4] As a consequence, one may rule out this mechanism in such photorearrangement reactions.

(4) Our present results allow us to elaborate on the standard model of the photochemistry of indoxazene (**1**), indazole (**3**), and isoazole-3-carboxylate (**5**) molecules. A knowledge of the conical intersection points of such species is of great importance in understanding their photoreactions, since it can affect the driving force of the photochemistry. For instance, **1** is excited vertically to the S_1 state. Then, radiationless decay from S_1 to S_0 occurs via a conical intersection (the direct pathway), which results in a rapid ring bond rotation. Starting from this conical intersection, the products of the phototranspositions as well as the initial reactant can be reached on a barrierless ground-state relaxation path. Indeed, the conical intersection mechanism found in this work gives a better explanation than the previously proposed internal cyclization−isomerization mechanism. Consequently, the conical intersection (the direct pathway) viewpoint has helped us to better understand the photochemical reactions and to support the experimental findings.[4,5]

It is hoped that the present work will stimulate further research into this subject.

Acknowledgment. I am grateful to the National Center for High-Performance Computing of Taiwan for generous amounts of computing time and the National Science Council of Taiwan for financial support. I also thank Professor Michael A. Robb, Dr. Michael J. Bearpark, (University of London, UK) and Professor Massimo Olivucci (Universita degli Studi di Siena, Italy) for their encouragement and support. Special thanks are also due to referees 1−3 for very helpful suggestions and comments.

Supporting Information Available: CASSCF/6-311G(d,p)-optimized geometries and CASSCF energies. This material is available free of charge via the Internet at http://pubs.acs.org.